Electronic Supplementary Information for Dalton Transactions

SUPPLEMENTARY MATERIAL

Structural, spectroscopic and magnetic properties of $M[R_2P(E)NP(E)R'_2]_2$ complexes, M = Co, Mn, E = S, Se and R, R' = Ph or ^{i}Pr. Covalency of M–S bonds from experimental data and theoretical calculations

Dimitrios Maganas,[a] Sarah S. Staniland,[b] Alexios Grigoropoulos,[a] Fraser White,[b]

Simon Parsons, [b] Neil Robertson, [b]* Panayotis Kyritsis [a]* and Georgios Pneumatikakis [a]

[a] Inorganic Chemistry Laboratory, Department of Chemistry, National and Kapodistrian University of Athens, Panepistimiopolis, GR-157 71, Athens, Greece.

[b] School of Chemistry, University of Edinburgh, King's Buildings, West Mains Road, Edinburgh, UK.

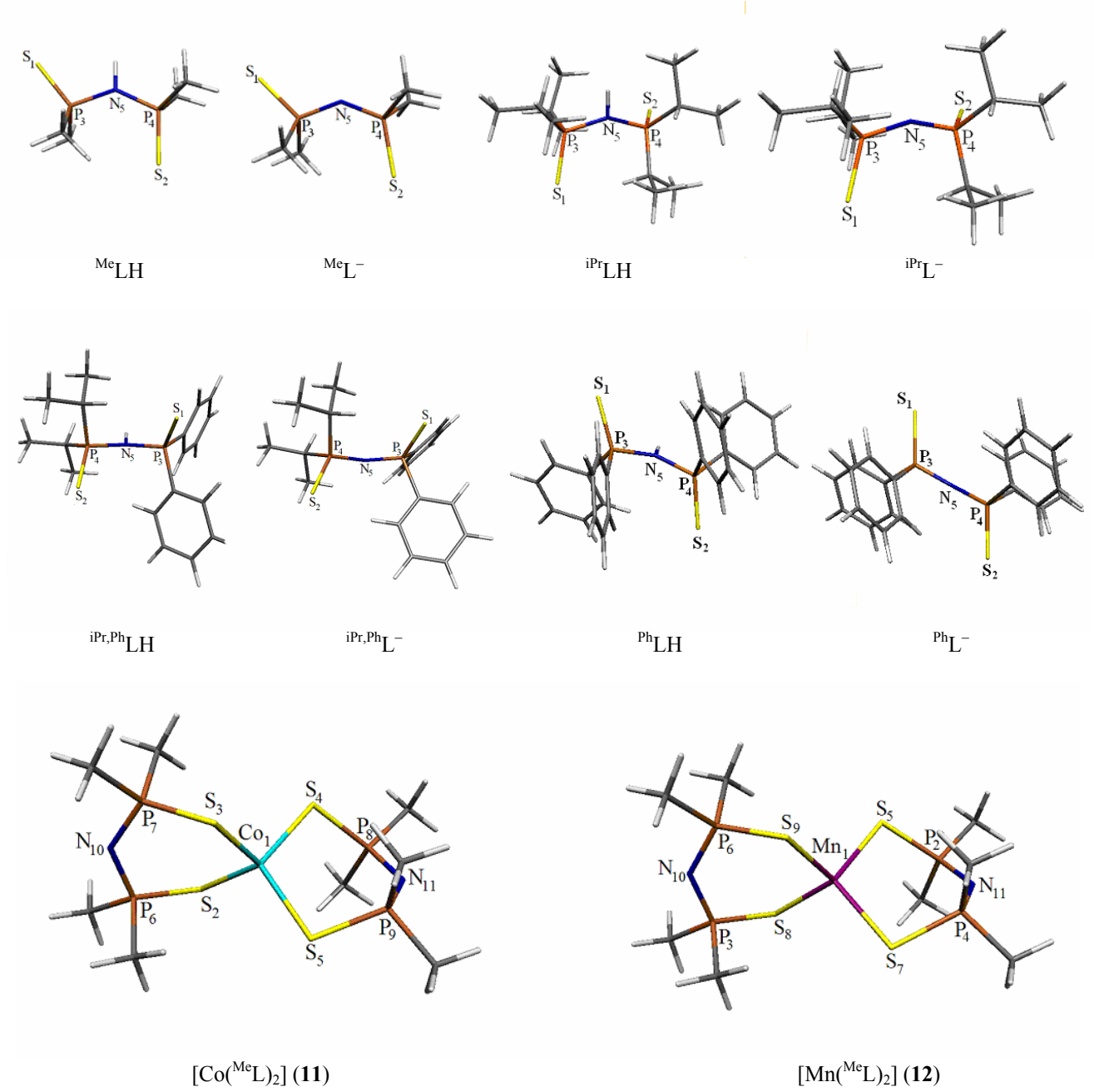

Fig. 1 Ground state optimized structures of the LH and L^- forms of the ligands, as well as of complexes **11** and **12**.

Table S1 Selected bond lengths (Å) and angles (°) for complexes **3, 5, 6** and **7**

Complex **3**			
Co(1)-S(2)	2.3061(4)	P(1)-N(1)	1.5826(12)
Co(1)-S(2)#1	2.3061(4)	P(2)-N(1)	1.5915(12)
Co(1)-S(1)	2.3356(4)	P(1)-C(11)	1.8109(15)
Co(1)-S(1)#1	2.3356(4)	P(1)-C(12)	1.8189(15)
P(1)-S(1)	2.0194(5)	P(2)-C(13)	1.8196(15)
P(2)-S(2)	2.0361(5)	P(2)-C(14)	1.8293(15)
S(2)-Co(1)-S(2)#1	110.69(2)	N(1)-P(1)-C(11)	106.70(7)
S(2)-Co(1)-S(1)	114.225(13)	N(1)-P(1)-C(12)	110.30(7)
S(2)#1-Co(1)-S(1)	110.599(13)	C(11)-P(1)-C(12)	103.81(6)
S(2)-Co(1)-S(1)#1	110.599(13)	N(1)-P(1)-S(1)	118.39(5)
S(2)#1-Co(1)-S(1)#1	114.225(13)	C(11)-P(1)-S(1)	108.67(5)
S(1)-Co(1)-S(1)#1	95.84(2)	C(12)-P(1)-S(1)	107.99(5)
P(1)-S(1)-Co(1)	98.553(18)	P(1)-N(1)-P(2)#1	139.21(8)
Symmetry transformations used to generate equivalent atoms: #1 -x,y,-z+3/2			

Complex **5**							
Mn(1)-S(1)	2.4464(6)	Mn(1)-S(2)	2.4379(6)	Mn(1)-S(3)	2.4404(6)	Mn(1)-S(4)	2.4432(6)
P(1)-N(1)	1.5906(17)	P(2)-N(1)	1.5940(17)	P(3)-N(2)	1.5914(17)	P(4)-N(2)	1.5905(17)
P(1)-S(1)	2.0270(7)	P(2)-S(2)	2.0271(7)	P(3)-S(3)	2.0311(7)	P(4)-S(4)	2.0291(7)
P(1)-C(11)	1.826(2)	P(1)-C(12)	1.831(2)	P(2)-C(13)	1.830(2)	P(2)-C(14)	1.831(2)
P(3)-C(16)	1.827(2)	P(3)-C(15)	1.834(2)	P(4)-C(17)	1.828(2)	P(4)-C(18)	1.829(2)
P(1)-N(1)-P(2)	138.20(11)	P(3)-N(2)-P(4)	139.87(12)	S(1)-Mn(1)-S(2)	109.59(2)	S(2)-Mn(1)-S(3)	109.37(2)
S(1)-Mn(1)-S(3)	107.35(2)	S(2)-Mn(1)-S(4)	108.16(2)	S(1)-Mn(1)-S(4)	111.53(2)	S(3)-Mn(1)-S(4)	110.82(2)
N(1)-P(1)-C(11)	106.21(9)	N(1)-P(1)-C(12)	111.04(9)	N(2)-P(3)-C(15)	110.65(10)	N(2)-P(3)-C(16)	106.38(9)
N(1)-P(2)-C(13)	106.14(9)	N(1)-P(2)-C(14)	110.88(9)	N(2)-P(4)-C(17)	105.95(9)	N(2)-P(4)-C(18)	111.29(9)
N(1)-P(1)-S(1)	119.08(7)	N(1)-P(2)-S(2)	118.65(7)	N(2)-P(3)-S(3)	118.36(7)	N(2)-P(4)-S(4)	119.14(7)
P(1)-S(1)-Mn(1)	105.60(3)	P(2)-S(2)-Mn(1)	105.57(3)	P(3)-S(3)-Mn(1)	105.56(3)	P(4)-S(4)-Mn(1)	104.75(3)

Complex **6**							
Mn(1)-S(1)	2.4578(10)	Mn(1)-S(2)	2.4394(10)	Mn(1)-S(3)	2.4515(10)	Mn(1)-S(4)	2.4348(10)
P(1)-N(1)	1.583(3)	P(2)-N(1)	1.590(3)	P(3)-N(2)	1.580(3)	P(4)-N(2)	1.593(3)
P(1)-S(1)	2.0142(12)	P(2)-S(2)	2.0286(13)	P(3)-S(3)	2.0156(12)	P(4)-S(4)	2.0269(13)
P(1)-C(11)	1.820(3)	P(1)-C(12)	1.815(4)	P(2)-C(15)	1.829(4)	P(2)-C(16)	1.828(4)
P(3)-C(13)	1.812(4)	P(3)-C(14)	1.817(3)	P(4)-C(17)	1.822(3)	P(4)-C(18)	1.836(4)
P(1)-N(1)-P(2)	140.8(2)	P(3)-N(2)-P(4)	141.2(2)	S(1)-Mn(1)-S(2)	110.02(4)	S(2)-Mn(1)-S(3)	116.80(4)
S(1)-Mn(1)-S(3)	96.91(3)	S(2)-Mn(1)-S(4)	107.07(4)	S(1)-Mn(1)-S(4)	117.01(4)	S(3)-Mn(1)-S(4)	109.22(4)
N(1)-P(1)-C(11)	110.21(16)	N(1)-P(1)-C(12)	106.46(17)	N(1)-P(2)-C(15)	104.60(17)	N(1)-P(2)-C(16)	112.08(16)
N(2)-P(3)-C(13)	106.62(17)	N(2)-P(3)-C(14)	110.28(16)	N(2)-P(4)-C(17)	112.27(17)	N(2)-P(4)-C(18)	105.12(17)
N(1)-P(1)-S(1)	118.50(12)	N(1)-P(2)-S(2)	116.96(12)	N(2)-P(3)-S(3)	118.55(12)	N(2)-P(4)-S(4)	117.29(12)
P(1)-S(1)-Mn(1)	95.98(4)	P(2)-S(2)-Mn(1)	99.35(5)	P(3)-S(3)-Mn(1)	96.81(4)	P(4)-S(4)-Mn(1)	100.93(5)

Complex **7**							
Mn(1)-Se(1)	2.5643(11)	Mn(1)-Se(2)	2.5691(11)	Mn(1)-Se(3)	2.5603(11)	Mn(1)-Se(4)	2.5344(11)
N(1)-P(1)	1.595(5)	N(1)-P(2)	1.589(5)	N(2)-P(3)	1.585(5)	N(2)-P(4)	1.589(5)
P(1)-Se(1)	2.1721(16)	P(2)-Se(2)	2.1721(15)	P(3)-Se(3)	2.1804(16)	P(4)-Se(4)	2.1727(16)
P(1)-C(11)	1.821(3)	P(1)-C(12)	1.821(3)	P(2)-C(13)	1.823(3)	P(2)-C(14)	1.814(3)
P(3)-C(15)	1.823(3)	P(3)-C(16)	1.818(3)	P(4)-C(17)	1.806(3)	P(4)-C(18)	1.818(3)
P(1)-N(1)-P(2)	132.2(3)	P(3)-N(2)-P(4)	136.3(3)	Se(1)-Mn(1)-Se(2)	112.81(4)	Se(2)-Mn(1)-Se(3)	113.75(4)
Se(1)-Mn(1)-Se(3)	108.01(4)	Se(2)-Mn(1)-Se(4)	102.90(4)	Se(1)-Mn(1)-Se(4)	105.44(4)	Se(3)-Mn(1)-Se(4)	113.65(4)
N(1)-P(1)-C(11)	104.9(2)	N(1)-P(1)-C(12)	110.1(2)	N(1)-P(2)-C(13)	109.9(2)	N(1)-P(2)-C(14)	105.1(2)
N(2)-P(3)-C(15)	110.8(2)	N(2)-P(3)-C(16)	104.4(2)	N(2)-P(4)-C(17)	107.6(2)	N(2)-P(4)-C(18)	108.1(2)
N(1)-P(1)-Se(1)	119.3(2)	N(1)-P(2)-Se(2)	117.6(2)	N(2)-P(3)-Se(3)	119.1(2)	N(2)-P(4)-Se(4)	119.42(19)
P(1)-Se(1)-Mn(1)	97.43(5)	P(2)-Se(2)-Mn(1)	92.77(5)	P(3)-Se(3)-Mn(1)	94.22(5)	P(4)-Se(4)-Mn(1)	102.67(5)

Table S2 Crystallographic data for complexes **3, 5, 6** and **7**

Complexes	**3**[a]	**5**[b]	**6**[c]	**7**[d]
Empirical formula	$C_{36}H_{48}Co_1N_2P_4S_4$	$C_{24}H_{56}Mn_1N_2P_4S_4$	$C_{37}H_{50}Cl_2Mn_1N_2P_4S_4$	$C_{48}H_{40}Mn_1N_2P_4Se4$
Fw	819.81	679.77	900.75	1139.48
Crystal system	Monoclinic	Triclinic	Triclinic	Triclinic
Space group	C 2/c	P -1	P 1	P -1
Crystal size,mm	0.42 x 0.25 x 0.18	0.30x0.71x0.52	0.20x0.21x0.30	0.35 x 0.15 x 0.15
Crystal shape and colour	Block, blue	Block, pink	Block, colourless	Block, colourless
A (Å)	12.6570(3)	9.2500(3)	9.9405(3)	13.7120(4)
B (Å)	15.6482(4)	12.7940(4)	10.2453(3)	13.8534(4)
C (Å)	21.4667(6)	16.3398(5)	11.2043(3)	14.1994(4)
A (deg)	90	79.2030(10)	96.560(2)	65.773(2)
B (deg)	103.356(2)	78.1480(10)	101.4900(10)	82.480(2)
Γ (deg)	90	69.0760(10)	100.4150(10)	70.427(2)
Volume ($Å^3$)	4136.69(18)	1753.93(10)	1086.35(5)	2317.53(12)
Z	4	2	1	2
P calc, Mg/m^3	1.316	1.287	1.377	1.633
Reflns collected/2Θmax	30143/61.0	17062/58.0	11470/114.4	41533/61.0
no reflections for shell	5771	7172	6648	6696
R1based on F/ goodness of fit	0.0327[a]/1.050	0.0384[b]/1.039	0.0421[c]/1.094	0.0688[d]/1.203
wR2 (F>4σ(F)	0.0901	0.0957	0.1035	0.1760
no of data/params/restr	6000/0/215	8180/0/316	11470/3/452	12970/0/436
Residual density, $eÅ^3$	0.575 / -0.237	0.595 and -0.394	0.485/-0.332	1.334 / -0.750

Weighted schemes:

a complex 3: w = 1/[\s^2^(Fo^2^) + (0.0501P)^2^ + 1.6942P] where P = (Fo^2^ + 2Fc^2^)/3 and 4997 data

b complex 5: w = 1/[\s^2^(Fo^2^) + (0.0470P)^2^ + 1.0297P] where P = (Fo^2^ + 2Fc^2^)/3 and 10848 data

c complex 6: w = 1/[\s^2^(Fo^2^) + (0.0482P)^2^ + 0.0000P] where P = (Fo^2^ + 2Fc^2^)/3 and 7228 data

d complex 7: w = 1/[\s^2^(Fo^2^) + (0.0369P)^2^ + 20.3487P] where P = (Fo^2^ + 2Fc^2^)/3 and 10646 data

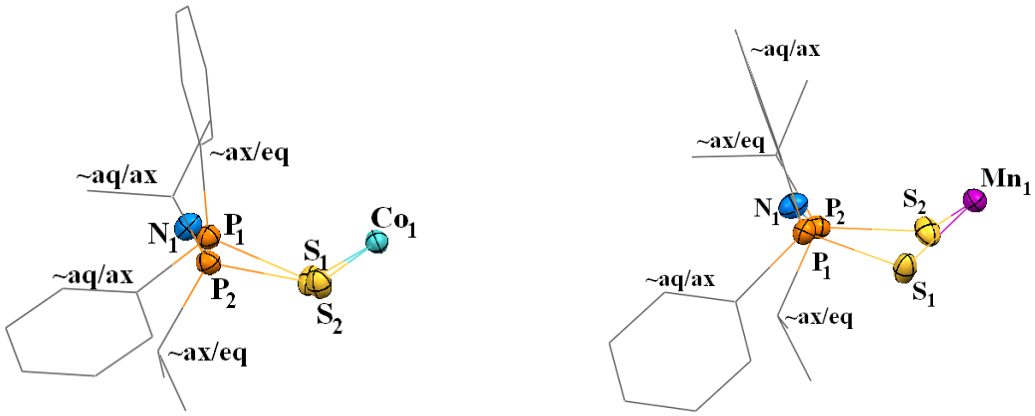

3 **6**

Fig. S1 Pseudo-boat conformation of the MSPNPS rings in complexes **3** and **6** with M (M = Co or Mn) and N at the apices and distorted axial-equatorial R-R′ interactions.

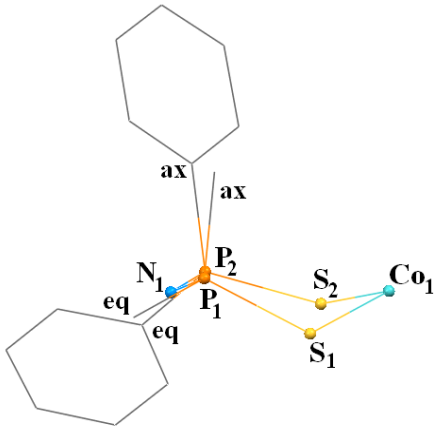

Fig. S2 Pseudo-chair conformation of the CoSPNPS ring in complex $Co[(SPPh_2)(SPMe_2)N]_2$ with the Co and N atoms at the apices and distorted axial-equatorial R-R′ interactions.

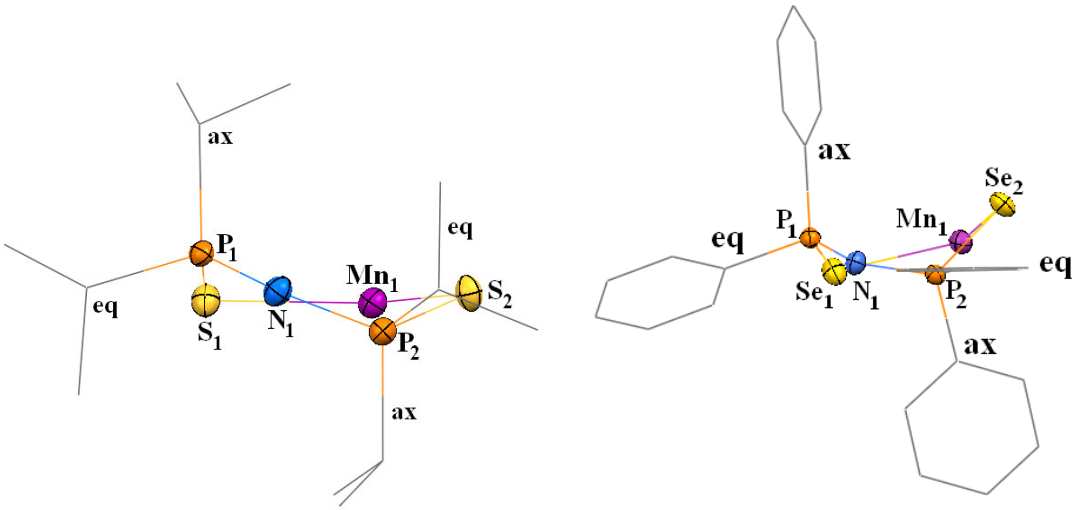

5 **7**

Fig. S3 Pseudo-boat conformation of the MnEPNPE (E = S or Se) rings in complexes **5** and **7** with the P and S atoms at the apices and axial-equatorial R-R interactions.

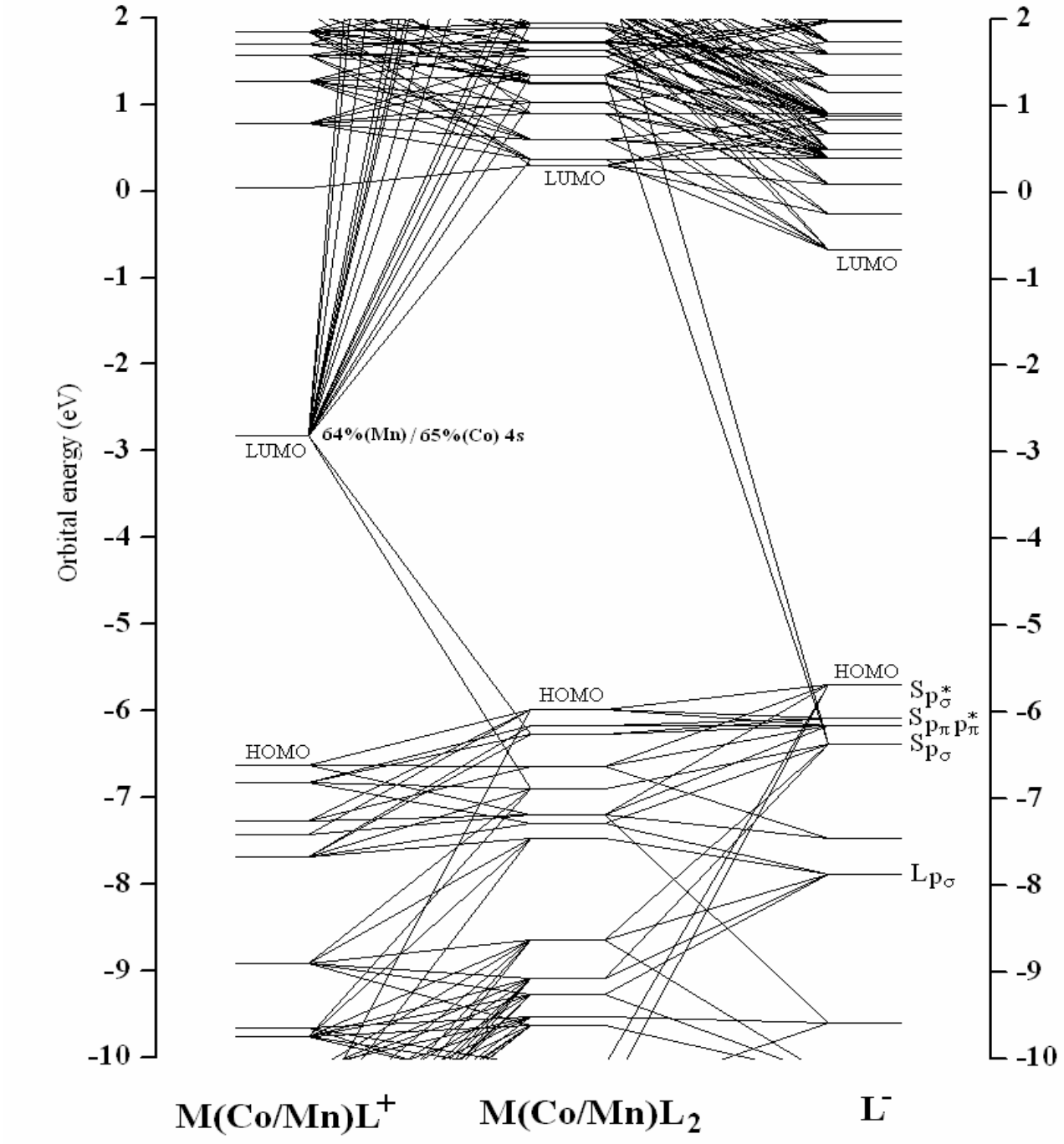

Fig. S4 α-spin orbital interaction diagram from an AOMix-CDA calculation on complexes **11** and **12**, with respect to a B3LYP/TZVP SP calculation on the ground state optimised structure. Molecular orbitals of the fragments ML^+ and L^- are shifted by 4.0 and –4.6 eV respectively. Lines connect all MO-FO orbital pairs with the corresponding MO-FO character greater than 2%.

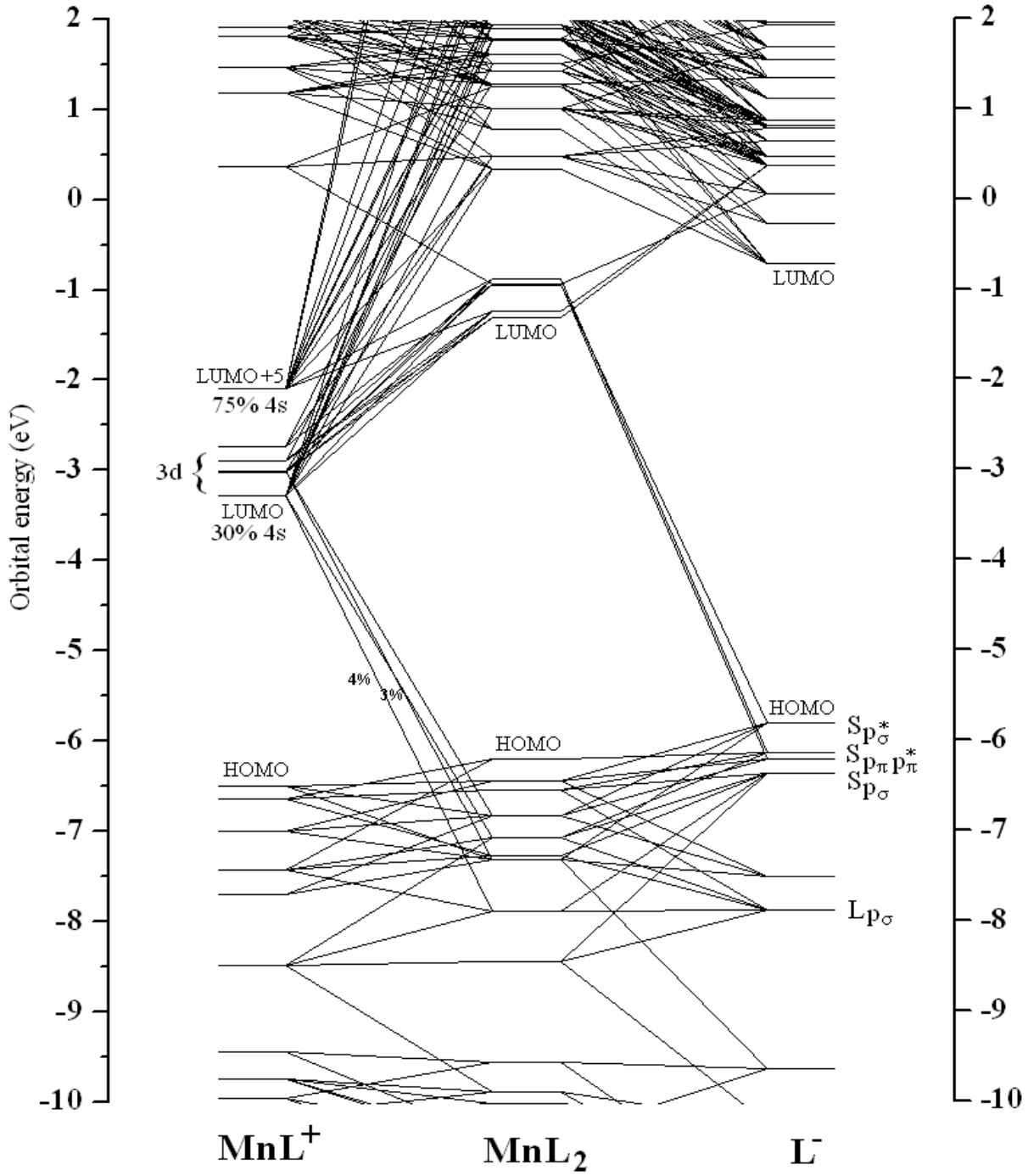

Fig. S5 b-spin orbital interaction diagram from an AOMix-CDA calculation on complex **12**, with respect to a B3LYP/TZVP SP calculation on the ground state optimised structure. Molecular orbitals of the fragments ML^+ and L^- are shifted by 4.0 and –4.6 eV respectively. Lines connect all MO-FO orbital pairs with the corresponding MO-FO character greater than 2%.

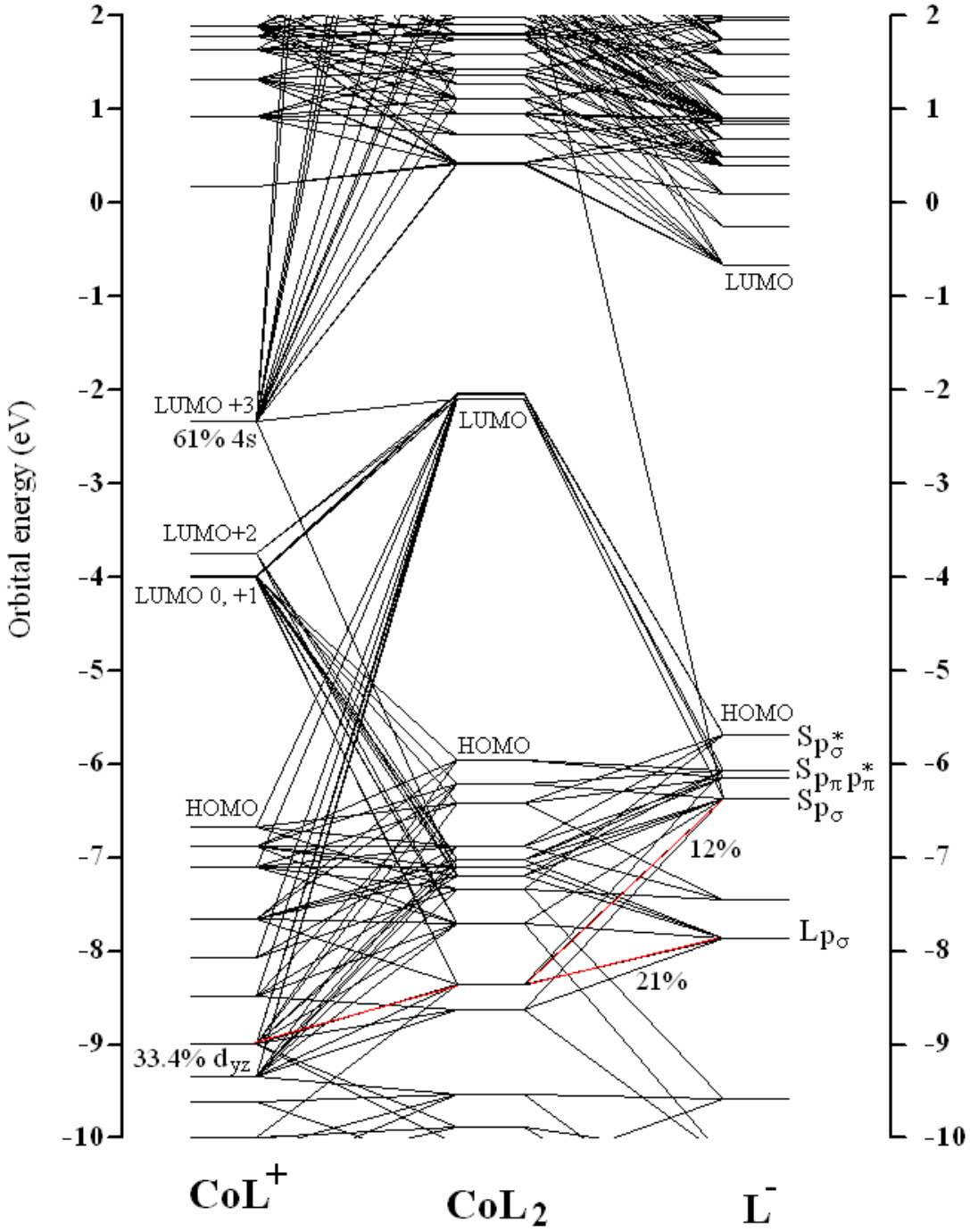

Fig. S6 b-spin orbital interaction diagram from an AOMix-CDA calculation on complex **11**, with respect to a B3LYP/TZVP SP calculation on the ground state optimised structure. Molecular orbitals of the fragments ML^+ and L^- are shifted by 4.0 and –4.6 eV respectively. Lines connect all MO-FO orbital pairs with the corresponding MO-FO character greater than 2%.